HHS Public Access

Author manuscript

Nat Chem Biol. Author manuscript; available in PMC 2010 March 01.

Published in final edited form as:

Nat Chem Biol. 2009 September ; 5(9): 680–687. doi:10.1038/nchembio.190.

Zebrafish chemical screening reveals an inhibitor of Dusp6 that expands cardiac cell lineages

Gabriela Molina[1,7,8], **Andreas Vogt**[2,6,8], **Ahmet Bakan**[3,8], **Weixiang Dai**[4], **Pierre Queiroz de Oliveira**[2], **Wade Znosko**[1], **Thomas E. Smithgall**[1,6], **Ivet Bahar**[3,6], **John S. Lazo**[2,6], **Billy W. Day**[4,5], and **Michael Tsang**[1,9]

[1]Department of Microbiology and Molecular Genetics, University of Pittsburgh, 3501 Fifth Ave, BST3-5062. Pittsburgh, PA 15213, USA.

[2]Department of Pharmacology and Chemical Biology, University of Pittsburgh, 3501 Fifth Ave, BST3-5062. Pittsburgh, PA 15213, USA.

[3]Department of Computational Biology, University of Pittsburgh, 3501 Fifth Ave, BST3-5062. Pittsburgh, PA 15213, USA.

[4]Department of Pharmaceutical Sciences, University of Pittsburgh, 3501 Fifth Ave, BST3-5062. Pittsburgh, PA 15213, USA.

[5]Department of Chemistry, University of Pittsburgh, 3501 Fifth Ave, BST3-5062. Pittsburgh, PA 15213, USA.

[6]Pittsburgh Molecular Libraries Screening Center, University of Pittsburgh, 3501 Fifth Ave, BST3-5062. Pittsburgh, PA 15213, USA.

Abstract

The dual specificity phosphatase 6 (Dusp6) functions as a feedback regulator of fibroblast growth factor (FGF) signaling to limit the activity of extracellular signal regulated kinase (ERK) 1 and 2. We have identified a small molecule inhibitor of Dusp6, (*E*)-2-benzylidene-3-(cyclohexylamino)-2,3-dihydro-1*H*-inden-1-one (BCI), using a transgenic zebrafish chemical screen. BCI treatment blocked Dusp6 activity and enhanced FGF target gene expression in zebrafish embryos. Docking simulations predicted an allosteric binding site for BCI within the phosphatase domain. *In vitro* studies supported a model that BCI inhibits Dusp6 catalytic activation by ERK2 substrate binding. A temporal role for Dusp6 in restricting cardiac progenitors and controlling heart organ size was uncovered with BCI treatment at varying developmental stages. This study highlights the power of *in vivo* zebrafish chemical screens to identify novel compounds targeting Dusp6, a component of the FGF signaling pathway that has eluded traditional high-throughput *in vitro* screens.

[9]Correspondence should be addressed to M.T. (tsang@pitt.edu) .
[7]Current address: SRI, Center for Advanced Drug Research, Harrisonburg, VA, USA.
[8]These authors contributed equally to this work.

AUTHOR CONTRIBUTIONS G.M., A.V., A.B., P.Q., W.D., W.A.Z., and M.T. performed experiments. G.M., A.V. A.B., T.E.S., J.S.L., I.B., B.W.D. and M.T., designed experiments and analyzed data. M.T. wrote the paper with help from A.V., A.B., T.E.S., J.S.L., B.W.D., and I.B.

Fibroblast Growth Factors (FGFs) are members of a large family of secreted glycoproteins that serve important functions in development, proliferation and cellular homeostasis1. These ligands bind to single-pass transmembrane proteins of the receptor tyrosine kinase class to activate multiple signaling pathways including the rat sarcoma homologue (RAS)/ mitogen-activated protein kinase (MAPK) cascade2. The wide-ranging biological roles of FGFs and the multitude of signaling pathways activated by this family of ligands suggest that FGF signaling must be tightly regulated. Dual specificity phosphatase 6 (Dusp6) (also named MAPK Phosphatase 3), Sproutys (Spry1-4) and Sef (similar expression to FGFs) proteins function as RAS/MAPK pathway feedback attenuators1,3. Through their concerted activities FGF signaling is adjusted to optimal levels in embryogenesis1,3. Sef and Spry proteins suppress RAS/MAPK signaling at multiple points within the pathway, while Dusp6 inhibits the pathway only by dephosphorylation of one class of the MAPK family, extracellular signal-regulated kinase (ERK)1. Sef, Dusp6 and Sprouty depletion in zebrafish or gene knock-out in mice have revealed the requirement for these proteins to limit FGF signaling during development and homeostasis1,4-6. The identification of small molecules that can reversibly modulate FGF signaling would provide useful tools to dissect the roles for this pathway in development that are not feasible with current genetic methods.

The zebrafish embryo is a vertebrate animal model well-suited for high-content small molecule screening7,8. Due to its small size, rapid development and ease of handling it is possible to identify compounds that affect developmental processes and chemical modulators of signaling pathways *in vivo*8,9. Previous zebrafish chemical screens have relied on the observations of phenotypes generated by exposure to small molecules. In one phenotypic screen, Dorsomorphin was identified as an inhibitor of Bone Morphogenetic Protein (BMP) as embryos exhibited axial patterning defects upon chemical treatment10. Subsequent studies utilizing Dorsomorphin in mice have revealed the importance of the BMP pathway in regulating iron metabolism10. Another example of the relevance of zebrafish screens was the discovery that Prostaglandin E2 is a key regulator of haematopoietic stem cell (HSC) homeostasis11. Their studies have shown that this pathway is conserved in vertebrates and provide the potential for using molecules to expand HSC to restore blood deficiencies in patients11.

The generation of transgenic reporter lines in zebrafish offers alternative *in vivo* tools for chemical screening. Reporters for FGF signaling have been generated and allow for the live visualization of signaling activity during early development12. In this study, we performed a chemical screen with an FGF reporter transgenic line and identified a small molecule, (*E*)-2-benzylidene-3-(cyclohexylamino)-2,3-dihydro-1*H*-inden-1-one (BCI, **1**), that hyperactivated FGF signaling. BCI was first described as a compound that suppressed NF-kB in cell-based luciferase reporter assays13. Our analyses revealed that BCI blocked Dusp6 activity in zebrafish embryos and in cultured cells. Molecular modeling predicted an energetically favorable site for BCI binding on the Dusp6 phosphatase domain and suggested a plausible allosteric mechanism of action, which was supported by *in vitro* assays. Using BCI as a chemical probe, we revealed that inhibition of Dusp6 activity during somitogenesis expanded cardiac progenitors at the expense of endothelial lineages. These studies suggest

that Dusp6 functions as an attenuator of FGF signaling in the cardiac field to regulate heart organ size.

Results

A zebrafish chemical screen identifies a modulator of FGF signaling

We previously described the generation of a transgenic zebrafish line, (*Tg(dusp6:EGFP)*^{pt6}) that expresses destabilized green fluorescent protein (d2EGFP) under the control of FGF signaling12. Using *Tg(dusp6:EGFP)* embryos as a biosensor for FGF signaling, we screened over 5000 diverse compounds assembled from chemical libraries for small molecule modulators of this pathway. Five transgenic embryos at 24 hours post fertilization (hpf) were arrayed into each well of a 96-well plate containing test compounds at 10 μM. d2EGFP intensity in treated embryos was visually analyzed and compared to vehicle control (0.5% DMSO) after 6-8 hours. BCI enhanced d2EGFP fluorescence in a concentration-dependent manner and was detected as early as 2 hours post treatment (Fig. 1a-c, BCI chemical structure shown in Fig. 1l). To confirm that BCI hyperactivated FGF signaling, we treated embryos prior to gastrulation (5hpf), and analyzed by whole mount *in situ* hybridization the expression of *ntl* (zebrafish *brachyury*), a known FGF target gene14. The expression of *ntl* was greatly expanded within the notochord and the tailbud at the 6-somite stage in BCI-treated embryos (Fig. 1d-f). Similarly, BCI treatment from the 1- to 10-somite stage resulted in a marked increase in expression of another FGF target gene, *dusp6*, as shown by the expansion of prospective mid-hindbrain boundary (MHB), rhombomere4 (r4) and the tailbud (Fig. 1g,h). The expanded brain structures were confirmed as BCI increased expression of *engrailed3* (*eng3*), which labels MHB, and *krox20*, which demarcates r3 and r5 identity, consistent with previous observations from FGF bead implantation studies (Fig. 1i,j)15. To further demonstrate that BCI treatment hyperactivated FGF signaling, we measured an increase in the expression of *sef* and *spry4* by semi-quantitative RT-PCR (Fig. 1k; n=3 for each gene)16-18. These results confirmed that BCI enhanced FGF signaling in the zebrafish embryo, resulting in the increased transcription of several FGF target genes.

We next determined the BCI structural features required to enhance FGF signaling. Two analogs, (*E*)-2-benzylidene-2,3-dihydro-1*H*-inden-1-one (BI, **2**) lacking the cyclohexylamino group, and 3-(cyclohexylamino)-2,3-dihydro-1*H*-inden-1-one (ICD, **3**) lacking the benzylidene group were synthesized (see Supplementary Materials for synthesis). The cyclohexylamino and benzylidene substituents were both required in enhancing d2EGFP fluorescence, as analogs lacking either group were inactive (Fig. 2c,d).

BCI inhibits Dusp6

To determine the mechanism for BCI's activity and to identify a potential target, we probed where this compound acts within the RAS/MAPK pathway. In BCI-treated transgenic embryos, increased d2EGFP expression was restricted to embryonic regions where FGFs are expressed (Fig 1b,c). Furthermore, BCI treatment did not induce d2EGFP expression in the MHB of *Tg(dusp6:EGFP);ace* mutant embryos, which are deficient in Fgf8 signaling (Fig. 3d)19. Thus BCI did not enhance FGF signaling in the absence of ligand. We reasoned that BCI could block a feedback attenuator of the FGF pathway, thereby resulting in a net

increase in transcription of target genes (Fig 3e). To test this model, we determined if BCI could rescue phenotypes generated by ectopic expression of FGF inhibitors, Spry4, Dusp6 and a dominant negative receptor, XFD in zebrafish (Supplementary Fig. 1a online)16,18. Injection of mRNA encoding *dusp6*, *spry4*, or *XFD* into 1-cell stage zebrafish embryos decreased *sef* expression (Fig. 3g,j,o and Supplementary Fig. 1c). The addition of 5 μM BCI to *dusp6*-injected embryos rescued *sef* expression to control levels or higher (Fig. 3h,o). In contrast, BCI treatment did not reverse the effects of *spry4* or *XFD* mRNA, suggesting that BCI directly inactivated Dusp6 (Fig. 3k,o and Supplementary Fig. 1d). To determine if BCI could inhibit other Dusps, we first characterized zebrafish *dusp5* and asked whether it could suppress FGF signaling similar to *dusp6*20,21. Dusp5 has been shown to dephosphorylate activated ERK (p-ERK) and ectopic expression of zebrafish *dusp5* inhibited *sef* transcription (Fig. 3m,o)22. In contrast to observations with Dusp6 mRNA microinjections, BCI had little or no effect in reversing the phenotype caused by Dusp5 over-expression (Fig. 3n,o). These observations indicated that BCI was specific for Dusp6. Although both Dusp6 and Dusp5 can dephosphorylate p-ERK and are highly conserved, their catalytic activities are quite different22,23. Dusp6 phosphatase activity is subject to substrate binding and can be catalytically stimulated by ERK interaction22,23. This substrate-induced catalytic activity has been described for several members of the Dusp family including Dusp1 (which is sensitive to BCI, as shown below), and Dusp423-25. In contrast, Dusp5 is constitutively activate and substrate binding has little consequence on catalytic rate22. Thus the difference we noted with the ability of BCI to rescue Dusp6 but not Dusp5 over-expression *in vivo* suggested that BCI might suppress the activation of Dusp6 associated with substrate binding.

Since Dusp6 directly dephosphorylates p-ERK, BCI should restore p-ERK levels in Dusp6 overexpressing cells. We tested this hypothesis in a cell-based chemical complementation assay26,27 in which HeLa cells were transiently transfected with Myc-tagged human Dusp6 (Dusp6-Myc), stimulated with 12-*O*-tetradecanoylphorbol-13-acetate (TPA, **4**), and immunostained with anti-c-Myc (Fig. 4a,b) and anti-p-ERK antibodies (Fig. 4c,d), respectively. Upon TPA treatment, the RAS/MAPK pathway was activated leading to strong p-ERK staining in non-transfected cells, while in cells expressing Dusp6-Myc (Fig. 4a), p-ERK staining was abolished (Fig. 4c, Dusp6-Myc cells traced in yellow). BCI treatment of Dusp6-Myc transfected cells restored p-ERK levels after TPA addition, suggesting that BCI directly suppressed Dusp6-Myc function (Fig. 4d, Dusp6-Myc traced in yellow). In this assay, BCI also inhibited human Dusp1, whose catalytic activity, like Dusp6, is induced by substrate binding (Fig. 4e)25. IC_{50} values for DUSP6 and DUSP1 inhibition from six independent experiments were 12.3 ± 4.0 μM and 11.5 ± 2.8 μM, respectively, consistent with hyperactivation of FGF signaling and d2EGFP expression at these concentrations in the zebrafish embryo (Fig. 4e). In contrast, treatment with ICD did not block Dusp6 or Dusp1 activity in the chemical complementation assays (Fig. 4e). Taken together, we have shown in biological systems BCI specifically inhibited Dusp1 and Dusp6, but not Dusp5.

We next addressed if BCI could directly inhibit Dusp6 activity in an *in vitro* pERK2 dephosphorylation assay. Recombinant Dusp6 completely dephosphorylated pERK2 *in vitro* as determined by immunoblotting with pERK specific antibodies (Fig. 4f, **lane 3**). Addition

of BCI prevented Dusp6-mediated pERK2 dephosphorylation as effectively as the generic tyrosine phosphatase inhibitor sodium orthovanadate (Fig. 4f, **lane 4** and **6, respectively**). ICD did not block Dusp6 activity supporting the conclusion that BCI directly inhibited Dusp6 (Fig. 4f, **lane 5**). Since many known small molecule phosphatase inhibitors exhibit low selectivity we determined whether BCI could suppress the phosphatase activity of several related phosphatases. BCI did not block Cdc25B (Cell division cycle 25B), PTP1B (Protein Tyrosine Phosphatase 1B) or Dusp3/VHR activity, implicating specificity of BCI is limited to a set of MAPK Phosphatases (Supplementary Fig. 2 online)

Computational modeling predicts a BCI binding site within Dusp6

Crystal structures of several Dusp catalytic domains have been determined 28-31. In each case, the phosphatase domain encompasses a five/six-stranded β-sheet surrounded by five α-helices. These structures enabled us to perform unbiased docking simulations32 to identify potential BCI binding sites (**Supplementary Methods** online). BCI was docked onto two different conformations of Dusp6 (MKP3): the low-activity form determined by X-ray crystallography (PDB ID: 1MKP)31 and the high-activity form obtained by homology modeling using ORCHESTRAR (Tripos, Inc., St. Louis, MO). From cluster analysis of the resulting BCI-bound conformations, we identified a number of potential binding sites on both the low- and high- activity forms (Fig. 5a, Supplementary Fig. 3 online). The most favorable site among them was further assessed by flexible docking33 using multiple Dusp6 conformations generated by anisotropic network model (ANM) analysis34 and homology modeling (**Supplementary Methods** online). BCI was predicted to preferentially fit within a crevice between the general acid loop and helix α7, rather than interacting directly with the catalytic residues Asp262, Cys293, or Arg299. At this putative binding site, a close interaction of BCI with the backbone of the general acid loop and the side-chains of Trp264, Asn335 and Phe336 was predicted (Fig. 5b). Further docking simulations using a homology model of Dusp1 showed that BCI-Dusp1 interactions were comparable to those with Dusp6 (Supplementary Fig. 4a online) rationalizing our observed activity data (Fig. 4e).

In the zebrafish microinjection assays, BCI inhibited ectopic expression of *dusp6* but not *dusp5*, exhibiting specificity toward certain members of this phosphatase family (Fig. 3). We compared the two-phosphatase crystal structures to understand how BCI can block Dusp6 but not Dusp5. Structural superposition of Dusp5 and Dusp6 displayed the particular crevice in Dusp6 that accommodates BCI binding is not accessible in Dusp5 (Fig. 5c)22,23,29. As a result, docking of BCI onto the same region of Dusp5 phosphatase domain resulted in energetically less favorable interactions (Supplementary Fig. 4b online). The relative positions of Asp262 and Asp232 in the respective phosphatases Dusp6 and Dusp5 differ by 5 Å after optimal superposition of the two structures, suggesting that their basal activities are determined by the relative location of these catalytic residues (Fig. 5c)29. It was postulated that substrate binding to Dusp6 induces a conformational shift that reorients Asp262 towards the phosphatase loop, thereby creating a high activity enzyme35. In support of this model, mutation of Asp262 to asparagine did not abolish basal phosphatase activity, but suppressed catalytic activation upon ERK binding31. To further understand BCI action on Dusp6 mechanistically, we explored Dusp6 dynamics by particularly focusing on the ANM modes that induce conformational changes at the general acid loop. Our analysis showed that

Dusp6 possesses an intrinsic, structure-induced tendency to suitably reorient its general acid loop to position Asp262 closer to the phosphatase loop (Movie 1 and Movie 2 online)36. Therefore, we proposed that BCI binding to the accessible crevice in the low-activity form effectively blocks the flexibility of this loop, thereby preventing the interaction of Asp262 with the other catalytic residues. Such constraints on functional motions are likely to inhibit Dusp6 activation induced by ERK binding.

BCI inhibits ERK2-mediated activation of Dusp6

To test these modeling predictions, we measured the dephosphorylation of a small molecule phosphatase substrate, 3-*O*-methylfluorescein phosphate (OMFP, **5**), by Dusp6 in the presence or absence of ERK2. Docking simulations predicted that BCI and OMFP could simultaneously bind within the phosphatase active site with OMFP interfacing with the core catalytic residues (Supplementary Fig. 5a online). This suggests that BCI would not block basal Dusp6 phosphatase activity toward OMFP. Indeed, at a concentration that inhibited ERK dephosphorylation *in vitro* (Fig. 4f), BCI did not inhibit basal Dusp6 activity (Supplementary Fig. 5b). Addition of ERK2 protein stimulated Dusp6 dephosphorylation of OMFP three-fold and this enhancement was significantly inhibited in the presence of BCI (57% inhibition) (Fig. 5d). Increasing the ratio of ERK2 to Dusp6 (10:1) in the activation assay resulted in a 7-fold enhancement that was also suppressed by the addition of BCI (30% inhibition) (Supplementary Fig. 5c). These data suggest that BCI is an allosteric inhibitor of Dusp6 that prevents the catalytic stimulation of phosphatase activity induced by substrate binding.

The role of Dusp6 and FGF in regulating heart size

The identification of a small molecule that blocks the biologically relevant activity of Dusp6 and Dusp1 allowed us to probe the requirement for these enzymes in later developmental processes. Given that BCI could potentially block related members of the Dusp family, we examined the expression of other *dusps* in zebrafish. Detailed expression analyses of several *dusps* have been described and include *dusp4, dusp1, dusp7, dusp5*, and *dusp22a* (see **Supplementary Methods** and Supplementary Fig. 6 online) (Thisse, B. & Thisse, C (http://zfin.org))20,21,37,38. Of these only Dusp6 functions as a feedback regulator of FGF/MAPK/ERK signaling and is expressed within the anterior lateral plate mesoderm, supporting the idea that this phosphatase plays a role in heart development. In early embryogenesis, Dusp6 is an important regulator of FGF signaling; knock-down with antisense morpholinos results in embryo polarity defects, which precludes the study of Dusp6's role in later development18. In contrast, small molecules permit the analysis at later stages of development due to rapid and transient perturbation of their biological targets.

Using BCI as a chemical probe, we asked how inhibiting Dusp6 activity would alter patterning and formation of the heart. The zebrafish heart develops from a small group of cardiac progenitor cells that can be identified by 5hpf within the mesodermal layer of the blastula stage embryo39,40. During gastrulation, cardiac progenitor cells undergo cellular migration to form two bilateral populations known as the anterior lateral plate mesoderm (ALPM) located just behind the MHB, and begin to express the transcription factors *nkx2.5* and *gata4*40,41. Studies have described a role for Fgf8 in zebrafish heart development. In

embryos harboring an *fgf8* mutation, both atria and ventricular cells are reduced42,43. In agreement with the notion that FGF signaling plays a role in stipulating heart size, ectopic expression of a constitutively activated FGF receptor (Fgfr1) during somitogenesis stages expanded cardiac tissue42. Therefore we used BCI to test if Dusp6 limits FGF signaling and restricts cardiac progenitors and heart organ size. In BCI-treated embryos a caudal expansion of *gata4* in the ALPM was observed (compare **Fig. 6a** to **6b**; 81%, n=16). The *gata4* caudal expansion of the ALPM corresponds to where cardiac progenitors are situated at the 10-somite stage. Examination of *nkx2.5* expression in BCI-treated embryos showed expanded cardiac progenitor pools as compared to DMSO-treated embryos, confirming a specific effect on heart precursors (compare **Fig. 6d** to **c**; 91%, n=11). While we noted an expansion of cardiac progenitors, it was not clear if this event was at the expense of other lineages. Recent studies have shown that there exists a repressive interaction between the vascular and hematopoietic precursors on cardiomyocyte progenitors that determine heart organ size44. We analyzed expression of *scl/tal1*, a gene that is expressed in endothelial and blood lineages located within the rostral domain of the ALPM in BCI-treated embryos from the 1-somite stage. Inhibition of Dusp6 resulted in a marked reduction in *scl* expression, suggesting that activation of FGF signaling expanded cardiac tissue at the expense of blood or endothelial progenitors (compare **Fig. 6f** to **6e**; 93%, n=15). Likewise, *etsrp*, a marker for vascular fate was also reduced in BCI-treated embryos (data not shown). The loss of endothelial and hematopoietic lineages was coupled with the concomitant expansion of cardiac *hand2* expression at the 10-somite stage (Fig. 6f; 32%, n=19). This surplus of cardiac progenitors was also noted at the 18-somite stage by an increase in cells positive for *cardiac myosin light chain 2* (*cmlc2*), which specifically labels differentiated cardiomyocytes (Fig. 6h; 81% n=16). To test whether the expansion of cardiac progenitors resulted in an increase in heart tissue, we analyzed treated embryos at larval stage. Embryos were treated at 40% epiboly with BCI or DMSO, followed by compound washout the next day and further incubated until the embryos reached 56hpf. In BCI-treated larvae, we noted a marked expansion in cardiac tissue (Fig. 6j,o). To define the critical period as to when Dusp6 activity limits heart organ size, we treated embryos at the 1- and 8-somite stages. We observed larger hearts at both time points, however the frequency was reduced in embryos treated at the later stage (Fig. 6o). *In situ* analysis with probes for *ventricular myosin heavy chain* (*vmhc*) and *cmlc2* confirmed that treated embryos exhibited enlarged hearts (Fig. 6l,n, and Supplementary Fig. 7 online). Expansion was particularly notable for ventricular tissue, known to be sensitive to Fgf8 signaling (Fig. 6l)42,43. These results indicate that inhibition of Dusp6 by a small molecule inhibitor can induce an expansion of myocardial progenitors that ultimately increase heart size.

Discussion

The zebrafish embryo offers distinct advantages over traditional *in vitro* and cell-based chemical screens. With the generation of transgenic FGF reporter lines, it is possible to screen for novel compounds that modulate this pathway *in vivo*. In addition, live embryo screens allow for the elimination of toxic compounds and molecules that evoke non-specific effects on embryo differentiation. From a modest screen of approximately 5000 compounds, we identified BCI, a small molecule that enhanced FGF signaling. Subsequent *in vitro*

phosphatase assays and docking simulations provided strong evidence that BCI suppressed the ERK-induced activation of Dusp6.

The identification of BCI allowed us to directly probe the role of Dusp6 in heart formation during a critical period when cardiac specific transcription factors begin to be expressed. The effects of BCI were consistent with studies when global activation of FGF signaling, which resulted in increased cardiac progenitors42. Treatment with BCI expanded the cardiac field at the expense of endothelial lineages. The increase in cardiac progenitors resulted in enlarged hearts, suggesting that FGF signaling must be tightly regulated during this period to allow for proper cardiac morphogenesis to occur. The role for Dusp6 in controlling heart organ size is likely conserved with other vertebrates as disruption of Dusp6 was recently found to cause enlarged hearts in mice6.

Previous large scale high-throughput screens for Dusp6 and Dusp1 inhibitors employed *in vitro* assays with artificial substrates. Because these assays do not faithfully recapitulate phosphatase activity in a biological context, no specific Dusp6 inhibitors with *in vivo* activity have been identified45. The phosphatase catalytic site is highly conserved across all tyrosine phosphatases and crystal structures have revealed shallow catalytic pockets. These structural features have further hampered the identification of specific small molecule phosphatase inhibitors46. Small molecules targeting Dusp1 identified from *in vitro* screens have exhibited promiscuous activity or lack biological activity47. However, with the identification of a chemical Dusp inhibitor, it should be possible to rationally design new molecules based on BCI to block substrate-induced Dusp function. This should offer highly specific compounds to probe the role of Dusps in development, and potentially provide novel agents for treatment of diseases that are dependent on FGF signaling such as wound repair and regeneration48,49.

METHODS

Zebrafish chemical screens

All procedures involving zebrafish were reviewed and approved by the University of Pittsburgh Institutional Animal Care and Use Committee. *Tg(dusp6:EGFP)*^{pt6} embryos were obtained by natural crossings and incubated at 28.5°C until they reached 24 hpf. Five transgenic embryos were placed into each well of a 96-well plate in 200 μl of E3, and a 0.5% DMSO solution was added along with compound from each library at 10 μM. The NCI diversity set (NCI/NIH), the Natural Products library (MicroSource Discovery Systems Inc.) and Phosphatase targeted set (ChemDiv Inc.) were screened in this study. (*E*)-2-Benzylidene-3-(cyclohexylamino)-2,3-dihydro-1*H*-inden-1-one (BCI; also known as NSC150117) was identified as a compound that enhanced fluorescence in treated transgenic embryos. Treated embryos were photographed under the same settings for exposure, gain and magnification for each picture using a MZFLIII (Leica) microscrope and fluorescent illumination for GFP using endow cube (Chroma Technology Corp.). Qimaging software and the Retiga Exi camera (Qimaging) were used to capture the images. Each experiment was repeated three times to show reproducibility of the assay and at least four of the five treated embryos exhibited the same phenotype.

Zebrafish mRNA microinjection

dusp6 and *XFD* mRNA for microinjection studies were generated as previously described18. Both Dusp5 and Spry4 ORFs were amplified by RT-PCR from 24 hpf zebrafish with the following primers:

Dusp5 Forward: 5′-AACTCGAGGCCATGAAGGTCTCCAGCATAGATTGCCG-3′

Dusp5 Reverse: 5′-AATCTAGATTAAGGCAGCGCAGTTATTGGACTC-3′

Spry4 Forward: 5′-ACTCGAGCCATGGAGTCAAGGGTTCCTCACCACATTC-3′

Spry4 Reverse: 5′-AATCTAGATCATGAGGCTTGTTTTTCTGGCTGAC-3′

Amplified PCR products were subcloned into pCS2+, sequenced verified and mRNAs were synthesized as described previously. Embryos were injected with 500 pg mRNA at the 1-2 cell stage, treated with 5 μM BCI at the 1000-cell stage and fixed at shield stage for *in situ* hybridization.

Chemical complementation assays in HeLa cells

These experiments were carried out essentially as described27. HeLa cells were obtained from ATCC (Manassas, VA) and maintained in a humidified atmosphere of 5% CO_2 at 37°C, Dulbecco's Minimum Essential Medium (DMEM) supplemented with 10% fetal bovine serum (FBS, HyClone), and 1% penicillin-streptomycin (Life Technologies, Inc.). Human c-Myc-Dusp6 (pSG5-PYST1) and Dusp1 (also known as CL100) were both kindly provided by Dr. Stephen Keyse (Cancer Research, UK)50. Full length Dusp1 was subcloned into pcDNA3.1 for ectopic expression in mammalian cells50. HeLa cells (2,000) were plated in the wells of a collagen-coated 384-well plate (Falcon Biocoat) in the presence of FuGene 6 (Roche Biosciences) and c-Myc-Dusp6 or c-Myc-Dusp1 as described27. After 20 h in culture, cells were treated in quadruplicate wells for 15 min with ten two-fold concentration gradients of BCI or ICD and stimulated for 15 min. with TPA (500 ng/ml). Cells were fixed and stained with Hoechst 33342 in 4% formaldehyde, permeabilized, and immunostained with a mixture of anti-pERK (1:200 dilution, Cell Signaling Technology) and anti-c-Myc (1:100 dilution, Santa Cruz Biotechnology) antibodies. Positive pERK and c-Myc-DUSP signals were visualized with AlexaFluor-594 (pERK) and Alexa-488 (c-Myc) conjugated secondary antibodies, respectively. Plates were analyzed by three-channel multiparametric analysis for p-ERK and c-Myc-DUSP intensities in an area defined by nuclear staining using the Compartmental Analysis Bioapplication on an ArrayScan II high-content reader (Cellomics). Restoration of ERK phosphorylation by BCI in Dusp6 overexpressing cells was quantified by Kolmogorov-Smirnov (KS) statistics as described previously using DUSP-transfected and vehicle treated control wells27. One thousand individual cells were gated for Dusp-Myc expression based on c-Myc immunostaining and analyzed for ERK phosphorylation. A pERK cumulative distribution function (cdf) was established for each condition and compared to a reference cdf from Dusp-Myc expressing and vehicle-treated cells. High KS values denote large differences in ERK phosphorylation levels compared with vehicle control and indicate suppression of Dusp activity. To quantify restoration of Erk phosphorylation in the Dusp expressing cells after compound treatment, KS values for

each condition were normalized to the average KS value from four wells transfected with Dusp1 or Dusp6 and treated with vehicle.

Detailed Material and Methods on *in vitro* phosphatase assays, molecular modeling, and chemical synthesis of BCI and related analogs are listed in Supplementary Methods online.

Supplementary Material

Refer to Web version on PubMed Central for supplementary material.

ACKNOWLEDGMENTS

The project described was supported in part by Award Number R01HL088016 to M.T. from the National Heart, Lung, and Blood Institute. The content is solely the responsibility of the authors and does not necessarily represent the official views of the National Heart, Lung, And Blood Institute or the National Institutes of Health. This work was also supported by NIH grants HD053287, CA52995, MH074411, and CA78039 and the Fiske Drug Discovery Fund. We thank N. Hukriede, M. Rebagliati and I. Dawid for critical reading of the manuscript. Michael S. Poslusney for assistance in the syntheses. The authors thank Dr Robert Schultz, Developmental Therapeutics Program, NCI, NIH for providing the NCI diversity set and samples of individual compounds.

Reference

1. Thisse B, Thisse C. Functions and regulations of fibroblast growth factor signaling during embryonic development. Dev Biol. 2005; 287:390–402. [PubMed: 16216232]
2. Dailey L, Ambrosetti D, Mansukhani A, Basilico C. Mechanisms underlying differential responses to FGF signaling. Cytokine Growth Factor Rev. 2005; 16:233–47. [PubMed: 15863038]
3. Tsang M, Dawid IB. Promotion and attenuation of FGF signaling through the Ras-MAPK pathway. Sci STKE. 2004; 2004:pe17. [PubMed: 15082862]
4. Abraira VE, et al. Changes in Sef levels influence auditory brainstem development and function. J Neurosci. 2007; 27:4273–82. [PubMed: 17442811]
5. Li C, Scott DA, Hatch E, Tian X, Mansour SL. Dusp6 (Mkp3) is a negative feedback regulator of FGF-stimulated ERK signaling during mouse development. Development. 2007; 134:167–76. [PubMed: 17164422]
6. Maillet M, et al. DUSP6 (MKP3) Null Mice Show Enhanced ERK1/2 Phosphorylation at Baseline and Increased Myocyte Proliferation in the Heart Affecting Disease Susceptibility. J Biol Chem. 2008; 283:31246–55. [PubMed: 18753132]
7. Vogt A, et al. Automated image-based phenotypic analysis in zebrafish embryos. Dev Dyn. 2009; 238:656–63. [PubMed: 19235725]
8. Zon LI, Peterson RT. In vivo drug discovery in the zebrafish. Nat Rev Drug Discov. 2005; 4:35–44. [PubMed: 15688071]
9. Peterson RT, Link BA, Dowling JE, Schreiber SL. Small molecule developmental screens reveal the logic and timing of vertebrate development. Proc Natl Acad Sci U S A. 2000; 97:12965–9. [PubMed: 11087852]
10. Yu PB, et al. Dorsomorphin inhibits BMP signals required for embryogenesis and iron metabolism. Nat Chem Biol. 2008; 4:33–41. [PubMed: 18026094]
11. North TE, et al. Prostaglandin E2 regulates vertebrate haematopoietic stem cell homeostasis. Nature. 2007; 447:1007–11. [PubMed: 17581586]
12. Molina GA, Watkins SC, Tsang M. Generation of FGF reporter transgenic zebrafish and their utility in chemical screens. BMC Dev Biol. 2007; 7:62. [PubMed: 17553162]
13. Callahan, JF.; Chabot-Fletcher, MC. Inhibitors of Transcription Factor NF-kB. US Patent Application. WO 99/65495. 1999.
14. Latinkic BV, et al. The Xenopus Brachyury promoter is activated by FGF and low concentrations of activin and suppressed by high concentrations of activin and by paired-type homeodomain proteins. Genes Dev. 1997; 11:3265–76. [PubMed: 9389657]

15. Maves L, Jackman W, Kimmel CB. FGF3 and FGF8 mediate a rhombomere 4 signaling activity in the zebrafish hindbrain. Development. 2002; 129:3825–37. [PubMed: 12135921]
16. Furthauer M, Reifers F, Brand M, Thisse B, Thisse C. sprouty4 acts in vivo as a feedback-induced antagonist of FGF signaling in zebrafish. Development. 2001; 128:2175–86. [PubMed: 11493538]
17. Tsang M, Friesel R, Kudoh T, Dawid IB. Identification of Sef, a novel modulator of FGF signalling. Nat Cell Biol. 2002; 4:165–9. [PubMed: 11802164]
18. Tsang M, et al. A role for MKP3 in axial patterning of the zebrafish embryo. Development. 2004; 131:2769–79. [PubMed: 15142973]
19. Reifers F, et al. Fgf8 is mutated in zebrafish acerebellar (ace) mutants and is required for maintenance of midbrain-hindbrain boundary development and somitogenesis. Development. 1998; 125:2381–95. [PubMed: 9609821]
20. Qian F, et al. Microarray analysis of zebrafish cloche mutant using amplified cDNA and identification of potential downstream target genes. Dev Dyn. 2005; 233:1163–72. [PubMed: 15937927]
21. Sumanas S, Jorniak T, Lin S. Identification of novel vascular endothelial-specific genes by the microarray analysis of the zebrafish cloche mutants. Blood. 2005; 106:534–41. [PubMed: 15802528]
22. Mandl M, Slack DN, Keyse SM. Specific inactivation and nuclear anchoring of extracellular signal-regulated kinase 2 by the inducible dual-specificity protein phosphatase DUSP5. Mol Cell Biol. 2005; 25:1830–45. [PubMed: 15713638]
23. Camps M, et al. Catalytic activation of the phosphatase MKP-3 by ERK2 mitogen-activated protein kinase. Science. 1998; 280:1262–5. [PubMed: 9596579]
24. Chen P, et al. Discordance between the binding affinity of mitogen-activated protein kinase subfamily members for MAP kinase phosphatase-2 and their ability to activate the phosphatase catalytically. J Biol Chem. 2001; 276:29440–9. [PubMed: 11387337]
25. Slack DN, Seternes OM, Gabrielsen M, Keyse SM. Distinct binding determinants for ERK2/p38alpha and JNK map kinases mediate catalytic activation and substrate selectivity of map kinase phosphatase-1. J Biol Chem. 2001; 276:16491–500. [PubMed: 11278799]
26. Vogt A, Lazo JS. Chemical complementation: a definitive phenotypic strategy for identifying small molecule inhibitors of elusive cellular targets. Pharmacol Ther. 2005; 107:212–21. [PubMed: 15925410]
27. Vogt A, Lazo JS. Implementation of high-content assay for inhibitors of mitogen-activated protein kinase phosphatases. Methods. 2007; 42:268–77. [PubMed: 17532514]
28. Almo SC, et al. Structural genomics of protein phosphatases. J Struct Funct Genomics. 2007; 8:121–40. [PubMed: 18058037]
29. Jeong DG, et al. Crystal structure of the catalytic domain of human DUSP5, a dual specificity MAP kinase protein phosphatase. Proteins. 2007; 66:253–8. [PubMed: 17078075]
30. Jeong DG, et al. Crystal structure of the catalytic domain of human MAP kinase phosphatase 5: structural insight into constitutively active phosphatase. J Mol Biol. 2006; 360:946–55. [PubMed: 16806267]
31. Stewart AE, Dowd S, Keyse SM, McDonald NQ. Crystal structure of the MAPK phosphatase Pyst1 catalytic domain and implications for regulated activation. Nat Struct Biol. 1999; 6:174–81. [PubMed: 10048930]
32. Morris GM, et al. Automated docking using a lamarckian genetic algorithm and an empirical binding free energy functions. Journal of Computational Chemistry. 1998; 19:1639–1662.
33. Jones G, Willett P, Glen RC, Leach AR, Taylor R. Development and validation of a genetic algorithm for flexible docking. J Mol Biol. 1997; 267:727–48. [PubMed: 9126849]
34. Atilgan AR, et al. Anisotropy of fluctuation dynamics of proteins with an elastic network model. Biophys J. 2001; 80:505–15. [PubMed: 11159421]
35. Owens DM, Keyse SM. Differential regulation of MAP kinase signalling by dual-specificity protein phosphatases. Oncogene. 2007; 26:3203–13. [PubMed: 17496916]
36. Bahar I, Chennubhotla C, Tobi D. Intrinsic dynamics of enzymes in the unbound state and relation to allosteric regulation. Curr Opin Struct Biol. 2007; 17:633–40. [PubMed: 18024008]

37. Brown JL, et al. Transcriptional profiling of endogenous germ layer precursor cells identifies dusp4 as an essential gene in zebrafish endoderm specification. Proc Natl Acad Sci U S A. 2008; 105:12337–42. [PubMed: 18719100]
38. Kudoh T, et al. A gene expression screen in zebrafish embryogenesis. Genome Res. 2001; 11:1979–87. [PubMed: 11731487]
39. Keegan BR, Meyer D, Yelon D. Organization of cardiac chamber progenitors in the zebrafish blastula. Development. 2004; 131:3081–91. [PubMed: 15175246]
40. Yelon D. Cardiac patterning and morphogenesis in zebrafish. Dev Dyn. 2001; 222:552–63. [PubMed: 11748825]
41. Chen JN, Fishman MC. Genetics of heart development. Trends Genet. 2000; 16:383–8. [PubMed: 10973066]
42. Marques SR, Lee Y, Poss KD, Yelon D. Reiterative roles for FGF signaling in the establishment of size and proportion of the zebrafish heart. Dev Biol. 2008; 321:397–406. [PubMed: 18639539]
43. Reifers F, Walsh EC, Leger S, Stainier DY, Brand M. Induction and differentiation of the zebrafish heart requires fibroblast growth factor 8 (fgf8/acerebellar). Development. 2000; 127:225–35. [PubMed: 10603341]
44. Schoenebeck JJ, Keegan BR, Yelon D. Vessel and blood specification override cardiac potential in anterior mesoderm. Dev Cell. 2007; 13:254–67. [PubMed: 17681136]
45. Ducruet AP, Vogt A, Wipf P, Lazo JS. Dual specificity protein phosphatases: therapeutic targets for cancer and Alzheimer's disease. Annu Rev Pharmacol Toxicol. 2005; 45:725–50. [PubMed: 15822194]
46. Bakan A, Lazo JS, Wipf P, Brummond KM, Bahar I. Toward a molecular understanding of the interaction of dual specificity phosphatases with substrates: insights from structure-based modeling and high throughput screening. Curr Med Chem. 2008; 15:2536–44. [PubMed: 18855677]
47. Lazo JS, et al. Novel benzofuran inhibitors of human mitogen-activated protein kinase phosphatase-1. Bioorg Med Chem. 2006; 14:5643–50. [PubMed: 16698271]
48. Gurtner GC, Werner S, Barrandon Y, Longaker MT. Wound repair and regeneration. Nature. 2008; 453:314–21. [PubMed: 18480812]
49. Lepilina A, et al. A dynamic epicardial injury response supports progenitor cell activity during zebrafish heart regeneration. Cell. 2006; 127:607–19. [PubMed: 17081981]
50. Dowd S, Sneddon AA, Keyse SM. Isolation of the human genes encoding the pyst1 and Pyst2 phosphatases: characterisation of Pyst2 as a cytosolic dual-specificity MAP kinase phosphatase and its catalytic activation by both MAP and SAP kinases. J Cell Sci. 1998; 111:3389–99. [PubMed: 9788880]

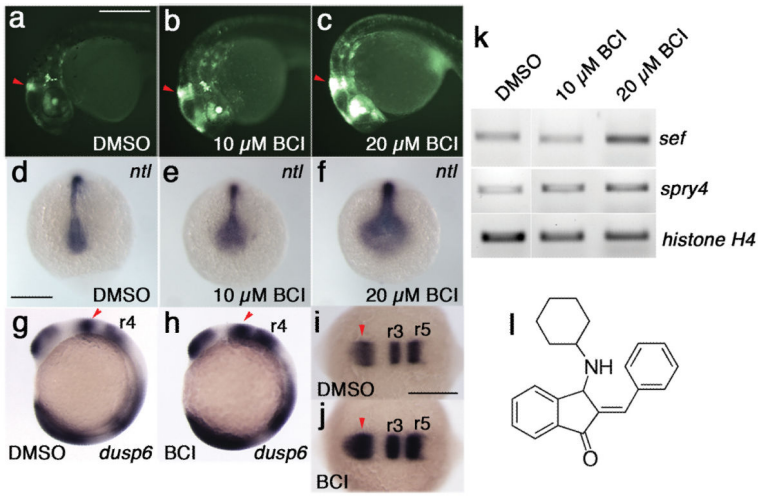

Figure 1. Identification of a small molecule that hyperactivates FGF signaling in zebrafish

(**a-c**) *Tg(dusp6:EGFP)*^{pt6} embryos at 30 hpf treated with BCI (**b,c**) exhibited increased d2EGFP fluorescence as compared to DMSO (**a**). (**d-f**) Embryos treated with BCI during gastrulation had expanded *ntl* expression at the 6-somite stage (**e,f**). (**g,h**) *dusp6* mRNA was increased in BCI treated embryos. Note that the MHB, r4 and somites showed stronger *dusp6* staining (**h**) than in DMSO treated (**g**). Red arrowheads demarcate the MHB. (**i,j**) BCI treatment during somitogenesis stages expanded the MHB and r3 and r5, as marked by *eng3* and *krox20* expression, respectively (**j**). (**k**) BCI treatment induced expression of the FGF target genes *sef* and *spry4* as measured by RT-PCR. Histone H4 served as RNA loading control. (**l**) The chemical structure of BCI. Scale bar, 250 μM

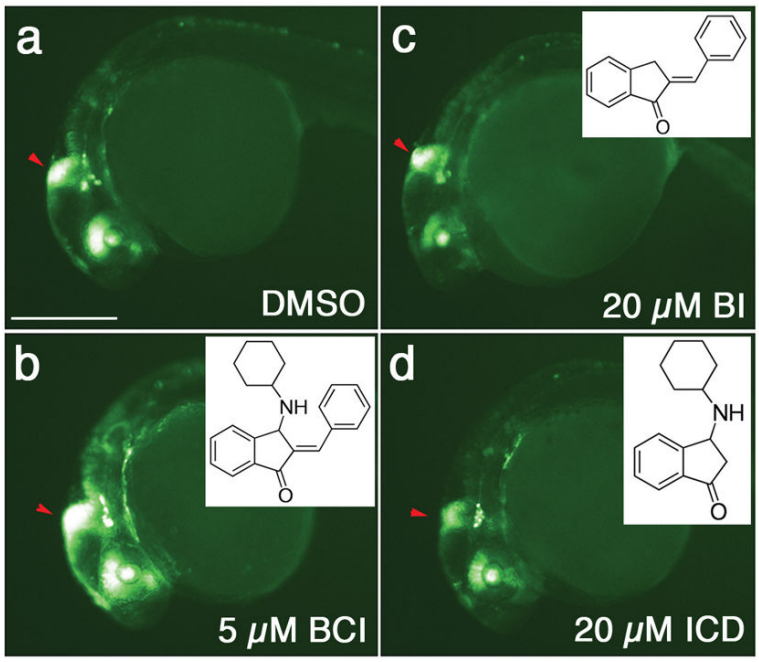

Figure 2. BCI structure-activity relationship studies

(**a-d**) Lateral views of 30 hpf *Tg(dusp6:EGFFP)*^{pt6} embryos treated with the compounds shown. d2EGFP fluorescence was enhanced in BCI-treated embryos (**b**), while related analogs, shown in inner panels, had no effect, even at four-fold higher concentrations (**c,d**). Red arrowheads marks MHB. Scale bar, 250 μM

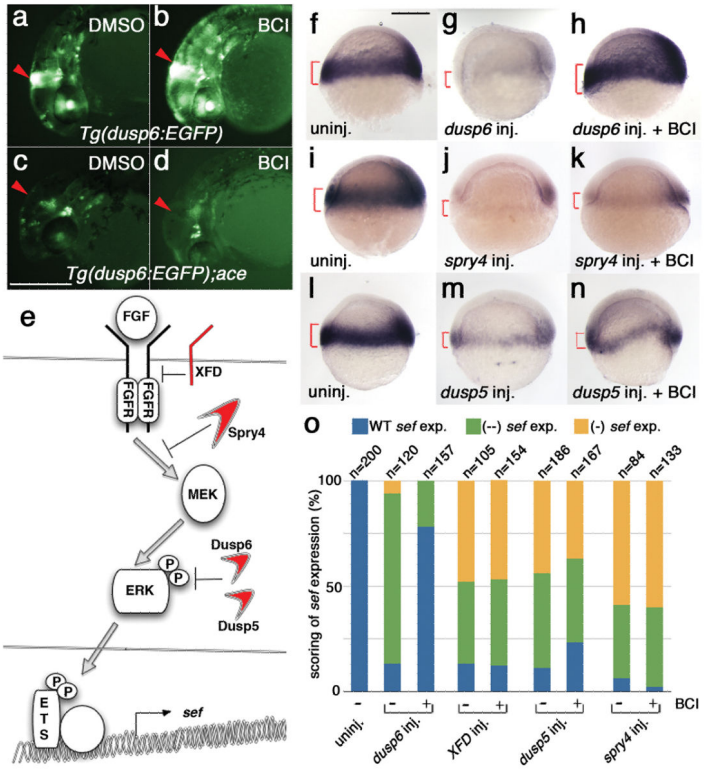

Figure 3. BCI does not hyperactivate FGF signaling in the absence of ligand and suppresses Dusp6 over-expression

(**a-d**) Lateral views of 30 hpf embryos. *Tg(dusp6:EGFP)*^{pt6} embryos (**a,b**) or *Tg(dusp6:EGFP)*^{pt6}*;ace* (**c,d**) were treated with BCI (10 μM). The *ace* mutants did not exhibit induction of d2EGFP within the MHB (red arrows) where FGF ligands are not present (**d**). (**e**) Schematic of FGF/RAS/MAPK pathway showing where XFD, Spry4 and Dusp act to block signaling. (**f-n**) Lateral views of shield staged embryos showing *sef* expression by *in situ* hybridization. Red brackets demarcate *sef* expression domain. Injection of *dusp6*, *spry4* or *dusp5* reduced *sef* expression (**g,j,m**). BCI treatment restored *sef* expression in *dusp6*-injected embryos (**h**), but not in embryos injected with *spry4* or *dusp5* (**k,n**). (**o**) Graph depicting injection and BCI treatment results. *Sef* expression in mRNA-injected embryos is represented by color bars that denote normal (WT) expression in blue, weaker (-) expression in yellow and absent (--) expression in green. Scale bar, 250 μM

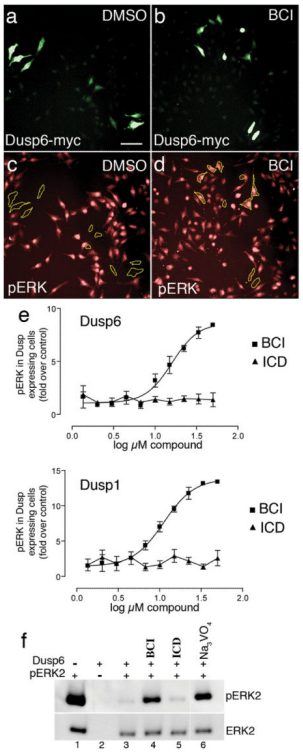

Figure 4. BCI directly inhibits Dusp6 in both chemical complementation and in pERK2 dephosphorylation assays

(**a-d**) Cell-based chemical complementation assay. TPA stimulation of HeLa cells induced ERK phosphorylation (red cells in **c,d**). In cells overexpressing Dusp6-Myc (green cells in **a**), p-ERK was abolished (**c**, green cells in **a** are outlined yellow cells). In the presence of BCI, pERK levels remained high (red cells in **d**), even in cells expressing high levels of Dusp6-Myc (outlined yellow cells in **d**). (**e**) Quantification of pERK levels in Dusp expressing cells. Cells expressing high levels of Dusp6 (upper panel) or Dusp1 (lower panel) were identified based on c-Myc immunostaining and analyzed for ERK phosphorylation using Kolmogorov-Smirnov (KS) statistics as described in Materials and Methods. pERK levels were normalized to Dusp transfected and vehicle treated cells. Data are the averages ± SD of quadruplicates from a single experiment that was repeated six times with similar results. (**f**) p-ERK2 *in vitro* dephosphorylation assay shows BCI (100 μM) specifically suppressed Dusp6 activity (lane 4) while a related analog, ICD (100 μM) was inactive (lane 5). Scale bar, 25μM

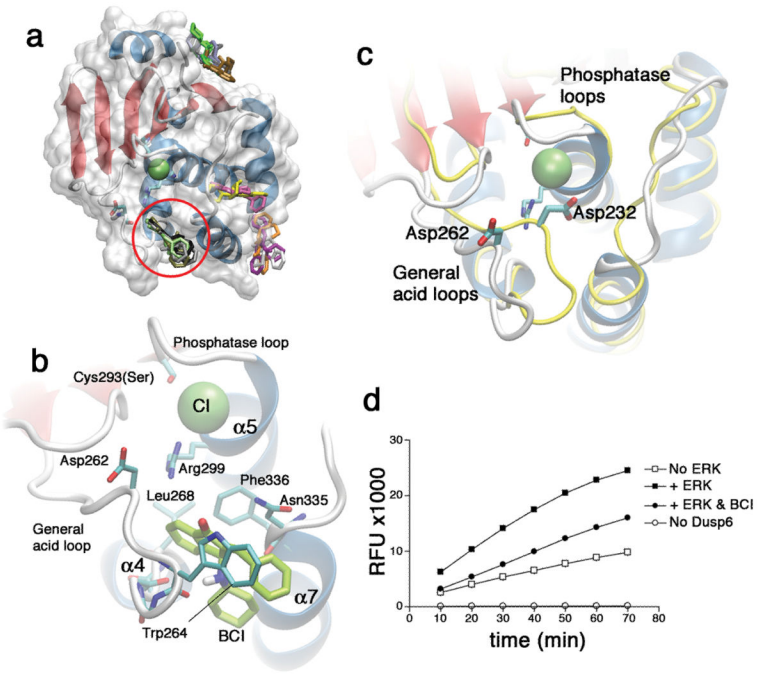

Figure 5. Modeling of BCI-Dusp6 interactions and *in vitro* testing of an allosteric inhibition mechanism

(**a**) Unbiased docking solutions for low-activity conformation of Dusp6 phosphatase domain. Each docking pose corresponding to a cluster of spatially close solutions is differently colored. Clusters in the vicinity of the active site are encircled. The catalytic cavity is distinguished by a chloride ion (green). (**b**) Close-up view of BCI (lime green) interactions. In addition to general acid loop backbone, BCI interacts with Trp262, Asn335 and Phe336 side-chains. (**c**) Superposition of Dusp5 (yellow) and Dusp6 (white) crystal structures showing that the catalytic acid, Dusp5-Asp232 is positioned approximately 5 Å closer to the catalytic pocket (phosphatase loop) than its Dusp6 counterpart (Dusp6-Asp262). (**d**) ERK2 stimulated Dusp6 dephosphorylation of OMFP and this induction was blocked by BCI. RFU, Relative Fluorescent Units were measured at excitation/emission wavelengths of 485/525nm.

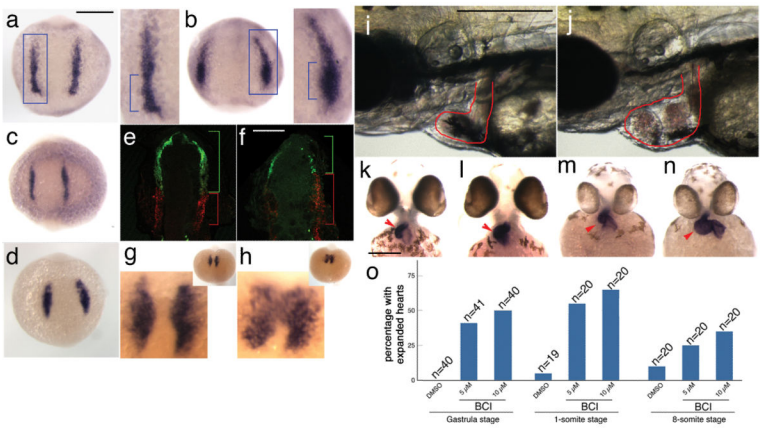

Figure 6. Dusp6 and FGFs regulate heart size

(**a-h & k-m**) *In situ* hybridization of embryos treated with BCI as indicated. (**a,b**) BCI treatment expanded *gata4* expression in the caudal ALPM (**b**); blue box and brackets mark ALPM and caudal cardiac domain, respectively. (**c,d**) BCI increased *nkx2.5* expression and expanded cardiac progenitor populations. (**e,f**) Fluorescent double *in situ* hybridization showing *scl* (green) and *hand2* (red) expression in BCI-treated embryos. Reduction of *scl* expression with a concomitant expansion of *hand2* in BCI treated embryos (**f**). Red and green bracket show expression domains. **(g,h)** *cmlc2* expression in 18-somite stage embryos showed an increase in cardiomyocytes in BCI-treated embryos. (**i,j**) Larvae at 56 hpf treated with BCI (from 40% epiboly for 8 hours) exhibited an enlarged heart. Red outline shows heart. These phenotypes correspond to expansion of *vmhc* (compare **l** to **k** and *cmlc2* (compare **n** to **m**) staining (red arrowheads). (**o**) Graph showing temporal inhibition of Dusp6 from gastrula to somitogenesis stages resulted in cardiac expansion. Scale bar, 250 μM

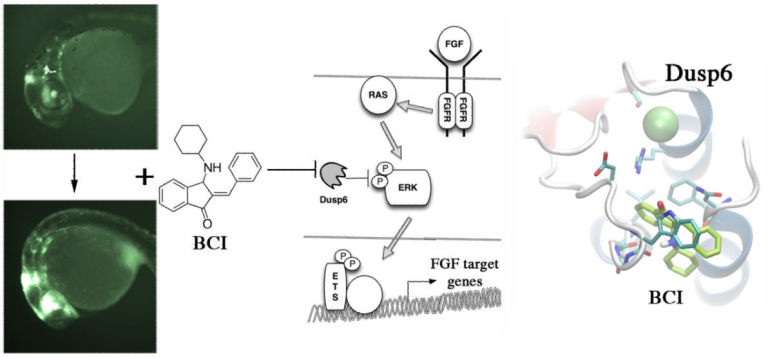

Figure 7.